Acoustic atomization induced pumping based on a vibrating sharp-tip capillary

Balapuwaduge Lihini Mendis¹, Ziyi He², Xiaojun Li¹, Jing Wang¹, Chong Li¹, Peng Li^{1*}

- C. Eugene Bennett Department of Chemistry, West Virginia University, Morgantown, WV. USA.
- 2. College of Veterinary Medicine, Huazhong Agricultural University, Wuhan, Hubei 430070, China.
 - * Correspondence and requests for materials should be addressed to P.L. (peng.li@mail.wvu.edu)

Abstract

Pumping is an essential component in many microfluidic applications. Developing simple, small footprint, and flexible pumping methods is of great importance to achieve truly lab-on-a-chip systems. Here, we report a novel acoustic pump based on the atomization effect induced by a vibrating sharp-tip capillary. As the liquid is atomized by the vibrating capillary, negative pressure is generated to drive the movement of fluid without the need of fabricating special microstructures or using special channel materials. We studied the influence of frequency, input power, internal diameter (ID) of the capillary tip, and liquid viscosity on the pumping flow rate, respectively. By adjusting the ID of the capillary from 30 μ m to 80 μ m and the power input from 1 V_{pp} to 5 V_{pp} , a flow rate range of 3-520 μ L/min can be achieved. We also demonstrated simultaneous operation of two pumps to generate parallel flow with tunable flow rate ratio. Finally, the capability of performing complex pumping sequences was demonstrated by performing bead-based ELISA in a 3D printed microdevice.

Keywords: Acoustofluidic pump; Atomization based pumping; Vibrating sharp-tip;

Introduction

For most microfluidic applications, fluid pumps are essential to achieve various fluid manipulations. Syringe pumps[1-3] or pneumatic pumps[4,5] are the most used pumps due to their wide availability and accurate flow rate control. However, the drawback of these pumps is their bulkiness that does not match the scale of most microfluidic devices, which hinders the development of lab-on a-chip systems with complex functionality. Therefore, developing miniaturized pumping methods is of great importance to further expand the application scope of microfluidic devices.

To date, a lot of efforts have been devoted to developing micropumps that are compatible with microfluidic devices. Based on the driving mechanisms there are two types of micropumps: passive pumps[6,7] and active pumps[8-10]. Passive pumps are based on surface tension or gravity to move fluids in a microchannel, which do not need peripheral equipment for the operations[7]. These pumping methods are suitable for simple applications that do not require complex fluid manipulation. For applications that need precise and on-demand fluid control, active pumps are preferred. Active pumps employ external actuation mechanisms for driving the fluid. Unlike the passive pumps, active pumps offer better flexibility in fluid manipulation. Typical active pumps include optically driven pumps[11,12], electric pumps[13,14], magnetic pumps[9,10], pneumatic membrane pumps, and acoustic pumps[15-34].

Among these pumping mechanisms, acoustic pumps have become increasingly important in recent years due to their small footprint, simple setup, and flexible operation. Early acoustic pumps induce deformation on channel walls thereby driving the fluid movement inside a microchannel[31]. Although this strategy is effective, its energy efficiency and the requirement of flexible channel walls limit its broad applications. Travelling Surface acoustic waves (TSAWs) induced body force and expansion force on liquid has also been used for fluid pumping. Tao et al.[15] reported a TSAW based pumping by applying RF signals to microfabricated interdigital

transducers (IDTs). The device was modified with hydrophobic coating for improving the pumping performance. They were able to achieve pumping flow rate in the range of 0.1 - 0.2 µL/min with a power consumption of 2-7 W. More recently, acoustic pumps based on acoustic streaming have also been reported[16,33,35]. Acoustic streaming is the stable fluid flow induced by the dissipation of acoustic energy to bulk fluid.[36,34,37] By controlling the direction and pattern of acoustic streaming, unidirectional movement of liquid can be achieved. It has been reported that sharpedge structures can induce strong acoustic streaming vortex for fluid pumping. Huang et al. [16] reported the first sharp-edge based pumping device by fabricating PDMS sharp-edge structures with a tilt angle to the channel wall, which breaks the symmetry of sharp-edge induced acoustic streaming leading unidirectional fluid low. This device achieved flow rates up to 8 µL/min at an input voltage of 50 V. Pavlic et. al[38] reports a microfluidic chip that has acoustically actuated sharp edges at the tip of channel opening that induces a flow in the microchannel made of silicon and glass. The oscillations of the sharp edges were able to induce a net fluid flow that reached up to 4.1 µL/min. In addition, SAW induced acoustic streaming can also be utilized for fluid pumping. Wu et al.[39] reported C shaped IDTs to generate localized acoustic streaming for fluid pumping. This method achieved flow rates in the range of 18.5 nL/min to 41.5 nL/min with a power consumption of 2-6 W. Although acoustic streaming-based pumps are simple and small footprint, these pumps are difficult to achieve complex fluid manipulations with multiple reagents due to the non-selective excitation of bulk acoustic vibration.

In this work, we present a novel acoustic pump that is based on the acoustic atomization effect. This method utilizes the fluid atomization effect generated by a vibrating sharp-tip capillary, which has been used as an ionization source for mass spectrometry analysis. In this work, we demonstrated that this phenomenon can be used as an efficient pumping method. As fluid is atomized at the capillary tip, a negative pressure is generated to the bulk fluid thereby creating unidirectional fluid flow. It has been reported that SAW induced atomization can induce

continuous fluid flow.[40.41,42] However, the requirement of SAW substrate and microfabricated electrodes limited their utility as a generic microfluidic pump. The present method allows independent control of each pumping unit, and the pumping performance is independent of the channel material and microstructures, which can be adopted by any microfluidic systems. We studied the relationship between the flow rates and various design and operational parameters including capillary geometry, input frequency, and amplitude. This pump achieved a flow rate range of 3-520 μ L/min. We demonstrated parallel flow streams in a microchannel by operating two pumps simultaneously. Finally, complex fluid operations were demonstrated by performing a complete bead-based ELISA protocol in a 3D printed microdevice.

MATERIALS AND METHODS

Reagents and materials

2.0 μ m amine modified polystyrene fluorescent orange latex beads were bought from Sigma Aldrich. The microparticle solution was prepared by mixing 5 μ L of the microsphere stock solution into 495 μ L of DI water. Rhodamine B powder was purchased from Sigma Aldrich. Rhodamine B fluorescent dye solution was prepared by mixing 1 mg of Rhodamine B powder with 10 mL of DI water and vortexed for complete dissolution. Water was purified using Milipore purification system (Beford, MA, USA). 5 μ m magnetic microparticles were bought from Sigma Aldrich. Streptavidin solution, Quanta Red enhanced chemifluorescent HRP substrate and phosphate buffered saline (PBS) were bought from thermos scientific. Quantikine ELISA commercial Activin A immunoassay kit was purchased from R&D Systems, Inc. USA. Glycerol was purchased from Sigma Aldrich. Solutions of different viscosities were prepared by diluting 50.00, 100.00, 150.00, 200.00 μ L, of Glycerol in DI water into a final volume of 600 μ L. Solutions of 4 different viscosities of 0.00115, 0.00153, 0.00209 and 0.00297 Ns/m² (1.2 cP, 1.5 cP, 2.1 cP, and 3.0 cP respectively) were made for viscosity experiment.

Device design and fabrication

The acoustically activated pulled tip glass capillary pump was fabricated based on our previous reports[43, 44]. Briefly, a piezoelectric transducer (7BB-27-4L0, Murata, Kyoto, Japan) and a pulled tip glass capillary were glued to the opposite ends of a microscope cover glass slide (24*60 mm purchased from VWR. The piezoelectric transducer was fixed to the glass slide using epoxy glue (5 min epoxy, Devcon). The puled tip glass capillary was made by pulling 0.4 mm ID capillary tubes purchased from Drummond Scientific Co. Broomall, PA 19008. (Drummond Scientific, Broomall, PA, USA) using a laser-based micropipette puller (P-2000, Sutter Instrument, Novato, CA, USA). The pulled-tip glass capillaries with their IDs in the range of 20 – 80 µm were fixed on to the opposite edge from the piezoelectric transducer of the glass slide using glass glue (Loctite Rocky Hill, CT, USA) with a 30-degree angle between the capillary and the shorter side of the glass slide with a distance to the corner ~5 mm as noted in Figure 1a. The angles and position of the capillary were optimized based on our previous work.[43]

All the microfluidic devices were first designed using SolidWorks. Then the devices were printed using Phrozen Sonic 4K resin 3D printer with a X-Y resolution of 35 µm. The UV light source wavelength of the printer is 405nm. The Nanoclear resin was purchased from Funtodo and SC-801 resin was purchased from Phrozen. After printing was complete, the printed device was removed from the build platform and was washed with Isopropanol to dissolve excess resin inside channels. After post-exposure process under UV (365nm) for 5 minutes, the device was glued to a glass slide (VWR, Radnor, PA, USA) using epoxy glue (5-minute epoxy, Devcon) to enhance the transparency of the device. The inlets and outlets of the device were connected to 0.034" I.D. * 0.060" O.D tubing purchased from Scientific Commodities. The device used for the on-chip beads-based ELISA comprises a well in the middle of the device to house the magnetic beads with a removable cover fixed to it. A magnet was used to immobilize the magnetic micro particles during the washing steps of ELISA.

Pump operation

The vibrating sharp-tip capillary pump was connected to the 3D printed microdevice via tubing. The whole system was then filled with water or other solutions manually. Then the outlet tubing was dipped in the reservoir containing the water or other desired solutions. The pumping was then activated and controlled using a Tektronix function generator (AFG1062) connected with an amplifier (LZY-22+, Mini-Circuits). The typical power input range is 1 – 5 Vpp, and the working frequency range is 90 - 100 kHz. During the pump operation, the flow rate was adjusted by changing the input power. To study the pumping flow rate, fluorescent particles were introduced to the microchannel. The movement of the particles was recorded using an epifluorescence microscope (Olympus IX 73) and a sCMOS camera (Hamamatsu Orca-Flash 4.0 LT+).

On-chip magnetic bead-based ELISA

 $2~\mu L$ of the 1 mg/mL streptavidin solution was mixed with 2.5 μL of 5 μm particle sized magnetic beads and 998 μL of PBS. Then the solution was incubated for 3 hours in the rotating stirring machine. Then the microparticles were washed 4 times with PBS (200 μL at each step). The streptavidin coated beads was then resuspended in 5 μL of PBS. 200 μL of the biotinylated capture antibody solution was added to the beads solution and was incubated at room temperature for 15 minutes followed by 3 washing steps with 200 μL of washing buffer at each step. Then the beads solution was mixed with 500 μL of 3% BSA and was incubated for 45 minutes under room temperature followed by 3 washing steps with 200 μL of washing buffer at each step. Then the beads were resuspended in 5 μL of PBS and was introduced into the 3D printed microdevice.

Inside the well of the sample device, 200 μ L of the sample mix (a mixture of 100 μ L of assay diluent and 100 μ L of 1000 pg/mL sample solution) was gradually pumped through the well using the stop flow method throughout the incubation time of 3 hours. For the control 200 μ L of only the assay diluent was pumped. Then the wash buffer was pumped 3 times across the well with 200 μ L at each step. During reagent introduction steps the beads were held in place using a

magnet that was placed under the device across from the well. And during incubation times the magnet was removed. Then 200 μ L of the detection antibody (Activin A conjugate) solution was pumped and was incubated for 1 hour followed by 4 washing steps using wash buffer with 200 μ L at each step. Then the substrate mix was prepared by mixing 200 μ L each from the Quantared stable Peroxide solution and Enhancer solution with 4 μ L of Quantared ADHP concentrate. Substrate mixture was pumped through sample and control devices (200 μ L each) and was incubated for 15 minutes before measuring the fluorescence intensity using

Results and discussion

Operation principle

In our previous works, we reported that a liquid filled sharp tip capillary can generate small liquid droplets, which can serve as an ionization source mass spectrometry analysis, termed vibrating sharp-edge spray ionization (VSSI) [43-47]. Typically, in VSSI mass spectrometry experiments, a syringe pump is used to ensure continuous sample loading. We also observed that as droplets are generated from the vibrating capillary, it can also induce fluid flow to sustain the ionization process. Here, we investigated whether this phenomenon could generate sufficient pressure to serve as an efficient pump for microfluidic devices. The pumping unit consist of a piezoelectric transducer, a glass slide, and a pulled tip capillary (Figure 1a). The piezoelectric transducer has a diameter of 27 mm, whereas the glass slide is 25*60 mm. The capillary tip was pulled to an ID 30 μm using a laser puller. After assembling the device, strong plume was observed when an RF signal was applied to the piezoelectric transducer (Figure 1b and Supporting video 1).

The microdevice tested in this study was fabricated using 3D printing. Based on the pumping mechanism of the present method, it is compatible with any microdevices regardless of its microfabrication methods or channel material. Here we chose a 3D printed device for testing as other acoustic pumps have not been applied to 3D printed devices due to the limitation of

printing resolution and channel material. The testing device has a main fluidic channel of 900 μ m * 950 μ m * 1.5 cm (width * height * length), one outlet connected to the pumping unit, and one inlet connected to a reagent reservoir (Figure 1c). It should be noted that the pulled-tip capillary was covered with a small tube for collecting aerosols. The whole fluidic channel and the pumping unit was first filled with water, and the outlet was connected to the reagent reservoir with Rhodamine B. When applying an RF signal of 94 kHz and 8 Vpp to the piezoelectric transducer, strong plume was observed at the tip of the capillary along with movement of Rhodamine B solution through the channel (Figure 2, Supporting Video 2). The flow rate was estimated to be ~200 μ L/min. This result indicated the feasibility of using the vibrating sharp-tip as a pumping unit for microfluidic devices.

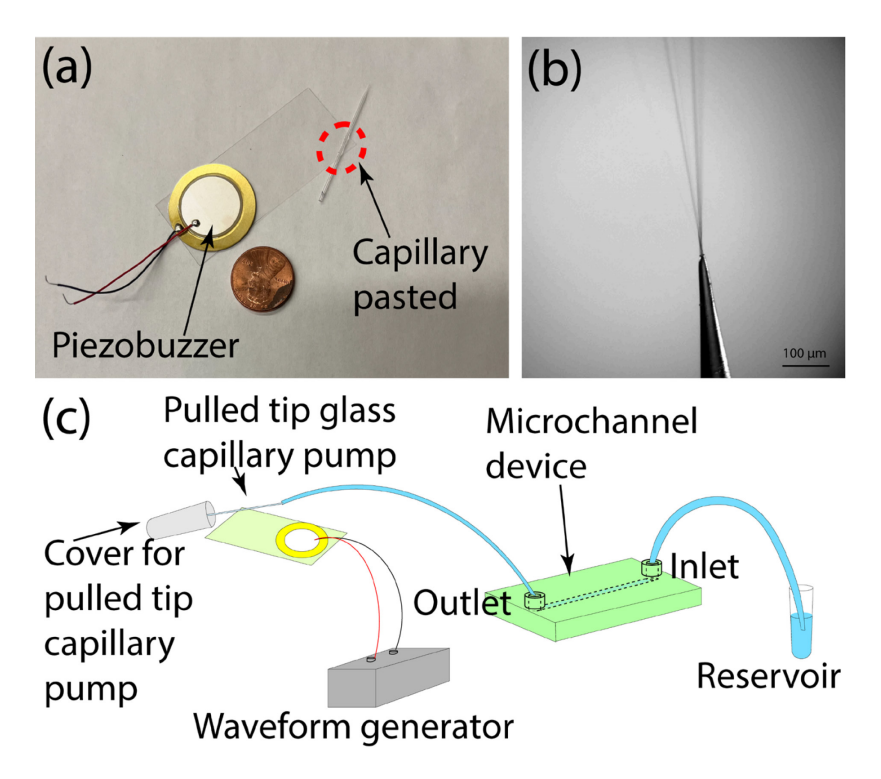
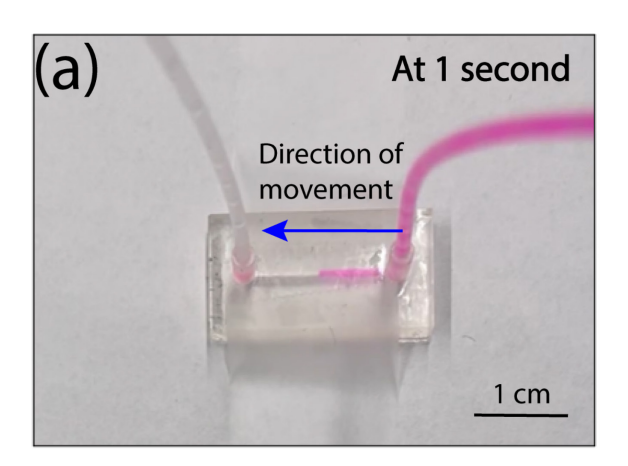


Figure 1(a) A vibrating sharp-tip capillary pumping unit. **(b)** Ejection of fluid from the vibrating sharp-tip capillary. **(c)**Schematic of the vibrating sharp-tip capillary pump based on microfluidic system.



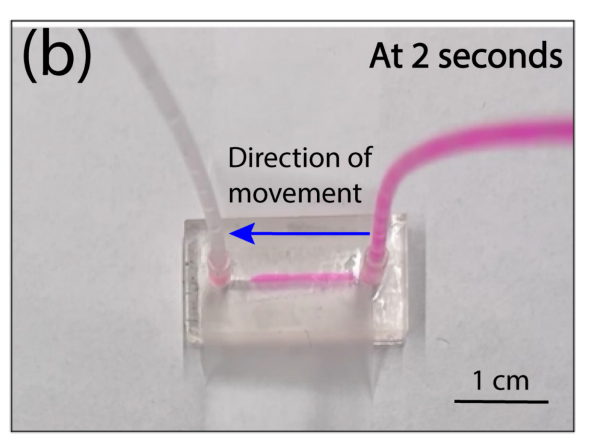


Figure 2(a) & (b) Movement of the Rhodamine B solution inside the channel driven by the vibrating sharp-tip capillary pump.

Characterization of important operational and design parameters on pumping performance

Next, we examined the factors that may affect the pumping flow rate. In this study, flow rate was calculated by measuring the flow velocity of 2 μ m fluorescent orange beads in the fluidic channel with a cross section of 900 μ m * 950 μ m. We first studied the impact of frequency on the pumping performance. The working frequency of the present system is dependent on the resonance frequency of the transducer, the device setup and its resonance frequency, and the damping in the system. We scanned frequency from 93 kHz to 99 kHz. As shown in Figure 3a, the pump can work under a broad range of frequency. In this work, we chose the frequency that generated the highest flow rate under the same power input as the optimal working frequency for the sharp-tip pump.

We also examined the relationship between the power input and the pumping flow rate. We tested a capillary with a tip ID of ~30 μ m at a frequency of 95 kHz. As shown in figure 3b, the flow rates increase with the increase in applied power. The relationship between the flow rate and input voltage is logarithmic instead of linear. We saw the flow rate increased from 5 μ L/min to 60 μ L/min, when the input voltage increased from 1 V_{pp} to 2 V_{pp} . Further increasing voltage from 2

Vpp to 5 Vpp only increased flow rate from 60 μ L/min to 85 μ L/min. To control the flow rate of the sharp-tip pump, a calibration curve needs to be established. It should also be noted that the sharp-tip pump has an onset voltage for the pumping phenomenon. For the capillary tested here, the onset voltage is ~0.9 V_{pp}. For voltages below this value, no atomization effect was observed, leading to no pumping for the microfluidic device.

Another factor that affects pumping flow rate is the ID of capillary tip. By controlling the parameters of the capillary puller, we fabricated pulled tip capillaries with IDs of 30 μ m, 50 μ m, 60 μ m, 70 μ m, 85 μ m, and measured their pumping flow rate under the same power input (4 V_{pp}). As shown in Figure 3c, the flow rate increases as the tip ID increases. Capillaries with large tip opening can generate more plume per unit time, which will translate to high flow rate based on the mass conservation law. It should be noted that as the tip size increases, the minimum flow rate increases as well. Therefore, for applications requiring low flow rates, smaller ID capillary is needed. In this work, the minimum flow rate achieved is ~3 μ L/min with a 30 μ m ID capillary. It is possible to achieve even lower flow rates with smaller ID capillaries. However, it is not recommended to use <30 μ m ID capillaries for general applications due to the increasing risk of tip clogging.

We also studied how fluid viscosity affects the pumping flow rate. Similar to other fluid pumps, it is also difficult to pump high viscosity fluids with the vibrating sharp-tip pump. As fluid viscosity increases, it becomes difficult to atomize the fluid, leading to decreased pumping efficiency. We prepared liquids samples with different viscosities of 1.2 cP, 1.5 cP, 2.1, and 3.0 cP using glycerol. Figure 3d showed the relationship between pumping flow rate and fluid viscosities. As fluid viscosity increased from 1.2 cP to 3.0 cP, the flow rate decreased from 54 μ L/min to 23 μ L/min .

We also examined the peak pressure that can be generated by the present pump. Since the 3D printed device used in above testing has a large cross section, the actual pressure requirement is low. To test capability of the present pumping method, we fabricated a PDMS

microchannel with a dimension of 600 μ m * 50 μ m * 1 cm (width * height * length). By tracking the fluorescent particle velocity, the sharp-tip pump achieved flow rates ranging from 0.5 – 40 μ L/min. Based on the Poiseuille's Law, the peak pressure generated by the sharp-tip pump is estimated to be ~1.1 kPa.

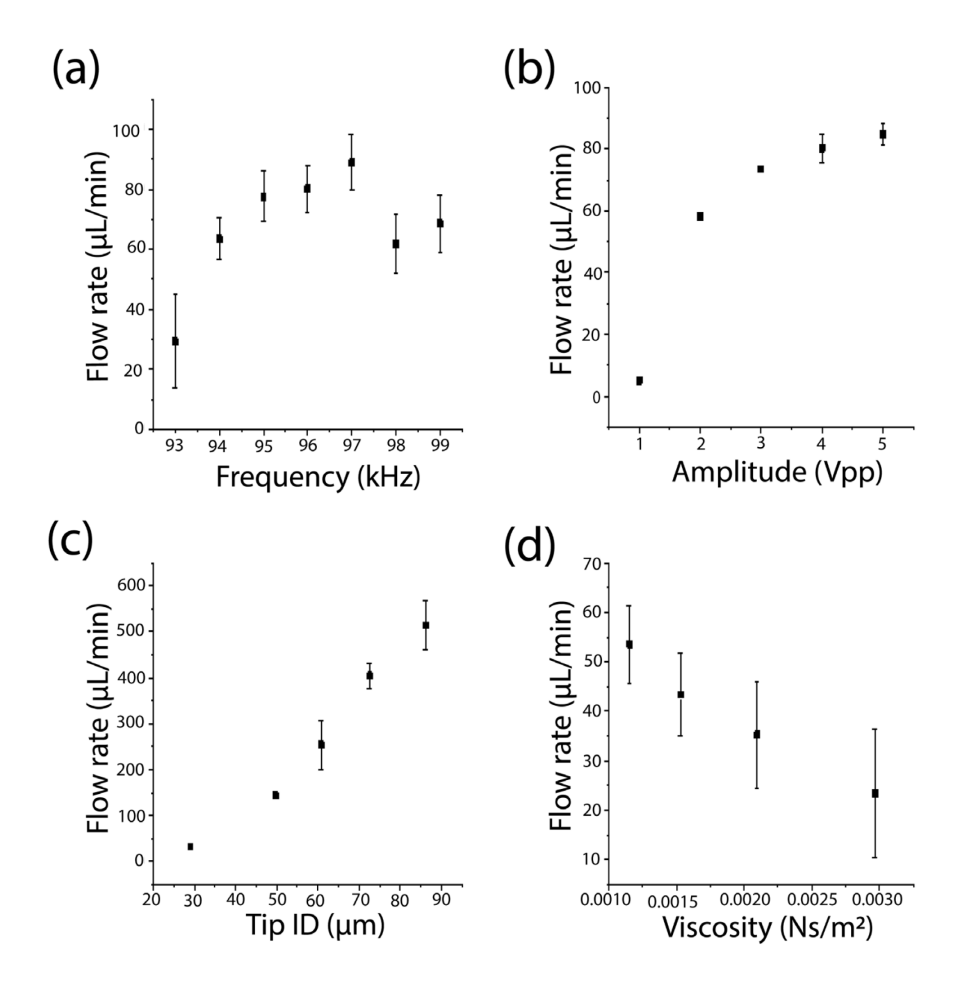


Figure 3 (a) Effect of input frequency in the range of 93-99 kHz on pumping flow rates; **(b)** Effect of input voltage on pumping flow rates; **(c)** Effect of the tip ID of the capillary on the flow rate; **(d)** Flow rate of solutions with different viscosities under the same input voltage and frequency. Error bars represent the standard deviation of three trials.

Multi-pump operations

The vibrating sharp-tip pump also allows operating multiple pumps simultaneously and independently. Here, we tested the operation of multiple vibrating sharp-tip capillary pumps with different reagents. For this study, we fabricated a microfluidic device with two inlets and two outlets as shown in figure 4(a). Two vibrating sharp-tip capillary pumps with tip ID ~ 80 µm were used. The two pumps were connected to the two outlets of the microchannel, respectively. Both pumps were operated at their optimal frequencies of 94 and 95 kHz, respectively. To observe the fluid flow from two pumps, the two inlets were connected to Rhodamine B reservoir and water reservoir, respectively. After turning on the two pumps simultaneously, we observed parallel streams of fluorescent solution (Rhodamine B) and water. When we increased the power input of Rhodamine B pump, the flow rate ratio between Rhodamine B and water increased, indicating that the parallel streams are controlled by the two pumps. The total flow rate was controlled to be ~400 µL/min to show two streams clearly without extensive mixing. By carefully designing the fluidic path, it is possible operate multiple pumps to deliver different reagents for chemical and biological analysis applications.

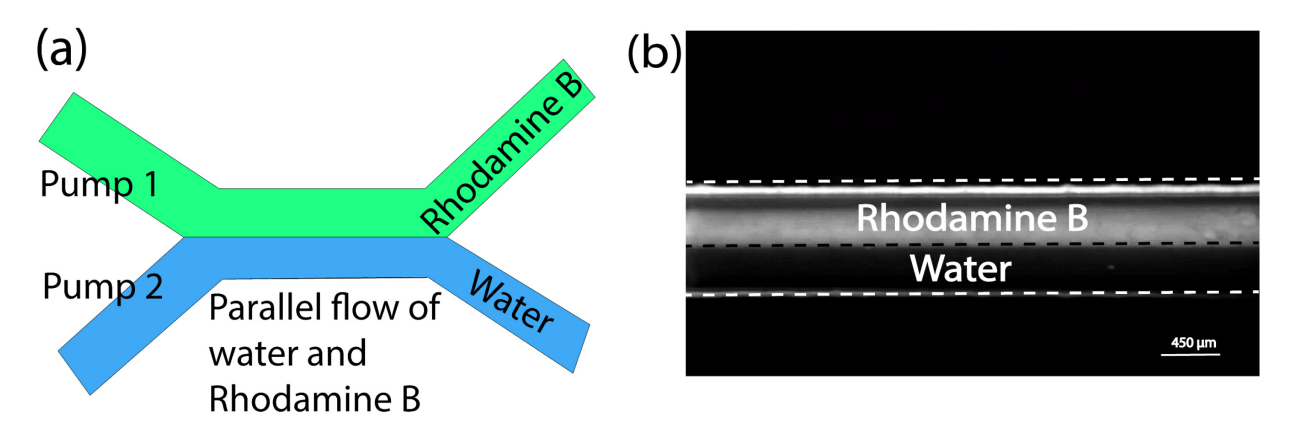


Figure 4 (a) schematic of dual vibrating sharp-tip capillary pump set up; **(b)** microscopic view of parallel flow of Rhodamine B and water generated by the simultaneous operation of the two pumps.

Performing sequential fluid operations to complete ELISA protocol.

Finally, we tested the vibrating sharp-tip capillary pump with complex fluid operations by performing a complete ELISA protocol. A complete ELISA protocol requires repeated cycles of reagent loading and washing. The vibrating sharp-tip capillary pump allows convenient loading of different reagents by simply swapping the reagent reservoirs connected to the micro-channel device. To perform on-chip ELISA, we designed a 3D printed microdevice with a center reaction chamber (Figure 5a). The center chamber is to hold capture antibody coated magnetic particles with a magnet. The suction pump was connected to the main outlet to provide fluid flow through the chamber. Two reagent inlets were employed for reagent loading and wash buffer loading, respectively. The reagent inlet was first connected to the sample solution, and later switched to different reservoirs in the order of detection antibody, and substrate as the assay progresses, whereas the wash buffer inlet was connected to the wash buffer reservoir throughout the assay. Finally, to control the flow of the system, a plug valve was placed near the reagent inlet to ensure the chamber can be washed properly without cross-contamination. Here we used a 1 ng/mL solution of Activin A standard as the target for the ELISA assay. The on-chip ELISA protocol is listed in Figure 5b. Once the capture antibody coated beads were introduced into the well, the sample solution was pumped through the channel device. After an incubation period of 3 hours, the washing buffer was pumped through the channel followed by the pumping of the detection antibody with a flow rate of µL/min. After 1 hour incubation, the beads were washed with ~1200 μL of ELISA washing buffer under a flow rate of 50 μL/min. Then the Quantared HRP substrate was pumped into the reaction chamber. After 15 min incubation, the fluorescence intensity was measured using Olympus IX 73 epifluorescence microscope with proper filter cubes. When loading reagents to the reaction chamber, the flow rate was set at 10 µL/min. During incubation, the flow was stopped. When washing the sample and detection antibody out of the device, the flow was increased to 30 µL/min and 50 µL/min, respectively, to ensure the complete removal of unbound reagents. As shown in Figure 5c, clear difference in fluorescence signals between the 1

ng/mL sample and the negative control sample was observed. This test showed the robustness of the present pumping method to perform complex fluid manipulations and operate over a long period of time. As the present pump is activated by RF signals, it will also be possible to achieve programmable fluid operations in the future.

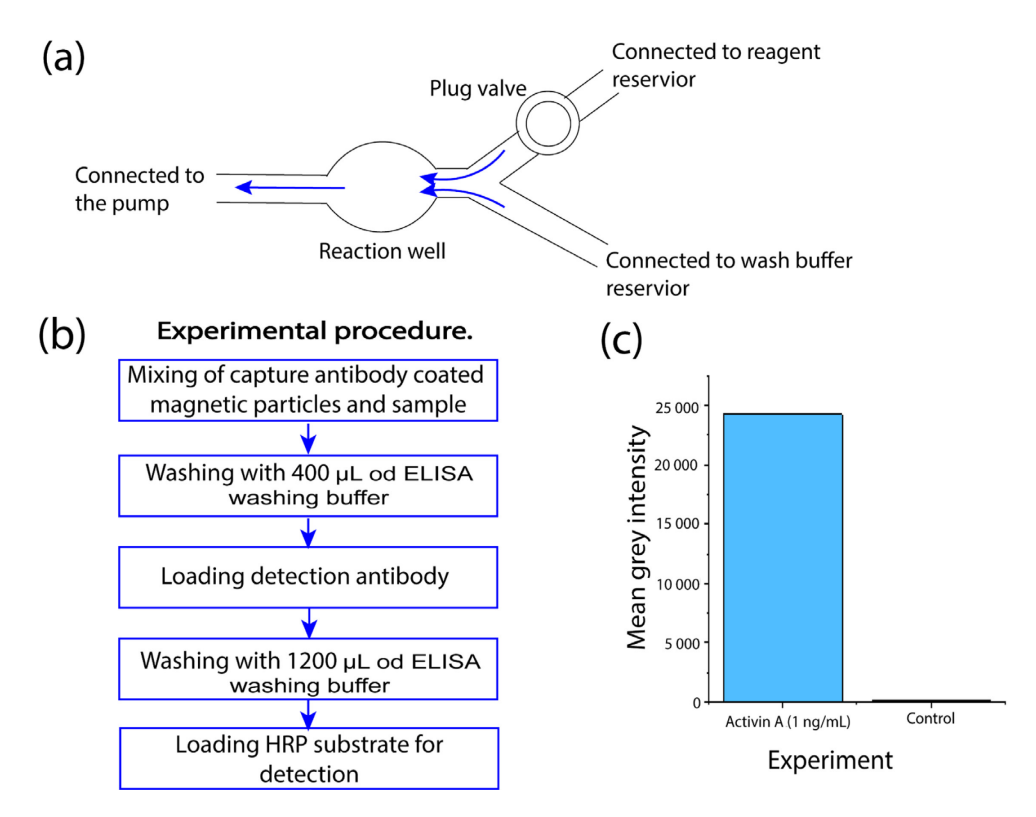


Figure 5(a) Schematic of the experimental setup for the on-chip bead-based ELISA; **(b)** the workflow of the on-chip bead-based ELISA; **(c)** Fluorescent intensity of 1 ng/mL Activin A sample and a control sample.

Conclusion

We reported a novel acoustic fluid pump based on the atomization phenomenon induced by a vibrating sharp-tip capillary. This pump is compatible with a wide range of microfluidic devices regardless of the channel material and fabrication methods. It is also simple and low cost to make. No special fabrication is necessary and each unit costs < \$1. In addition, the low power consumption of the present method (~2-40 mW) makes it possible to be activated by simple signal

generation and amplification circuits with battery power. Collectively, these features make this method a good candidate to perform complex and programmable fluid operations in point-of-care (POC) settings. To achieve the highest energy efficiency, we utilized the atomization phenomenon for fluid pumping. The potential issue with the atomization effect is the extra stress exerted on biological cells. Further studies are necessary to examine the present method allows recovery of cells with high viability and minimal stress. In the future work, we will also explore the pumping phenomenon by inserting the vibrating sharp-tip capillary into a liquid to avoid the generation of aerosols and improve its biocompatibility.

Acknowledgement

This work was supported in part by the National Science Foundation (ECCS-2144216).

References.

- 1. Yu, N.; Liu, Y.; Wang, S.; Tang, X.; Ge, P.; Nan, J.; Zhang, J.; Yang, B. Pressure-Controlled Microfluidic Sub-Picoliter Ultramicro-Volume Syringes Based on Integrated Micro-Nanostructure Arrays. *Lab. Chip* **2019**, *19*, 3368–3374.
- 2. Li, Z.; Mak, S.Y.; Sauret, A.; Shum, H.C. Syringe-Pump-Induced Fluctuation in All-Aqueous Microfluidic System Implications for Flow Rate Accuracy. *Lab. Chip* **2014**, *14*, 744.
- 3. Zhao, Z.; Yang, Y.; Zeng, Y.; He, M. A Microfluidic ExoSearch Chip for Multiplexed Exosome Detection towards Blood-Based Ovarian Cancer Diagnosis. *Lab. Chip* **2016**, *16*, 489–496.
- 4. Choi, J.-W.; Lee, S.; Lee, D.-H.; Kim, J.; deMello, A.J.; Chang, S.-I. Integrated Pneumatic Micro-Pumps for High-Throughput Droplet-Based Microfluidics. *RSC Adv* **2014**, *4*, 20341–20345.
- 5. Clime, L.; Brassard, D.; Geissler, M.; Veres, T. Active Pneumatic Control of Centrifugal Microfluidic Flows for Lab-on-a-Chip Applications. *Lab. Chip* **2015**, *15*, 2400–2411.
- 6. Walker, G.M.; Beebe, D.J. A Passive Pumping Method for Microfluidic Devices. *Lab. Chip* **2002**. *2*. 131.
- 7. Marimuthu, M.; Kim, S. Pumpless Steady-Flow Microfluidic Chip for Cell Culture. *Anal. Biochem.* **2013**, *437*, 161–163.
- 8. Gu, C.; Jia, Z.; Zhu, Z.; He, C.; Wang, W.; Morgan, A.; Lu, J.J.; Liu, S. Miniaturized Electroosmotic Pump Capable of Generating Pressures of More than 1200 Bar. *Anal. Chem.* **2012**, *84*, 9609–9614.
- 9. Cho, Y.-K.; Lee, J.-G.; Park, J.-M.; Lee, B.-S.; Lee, Y.; Ko, C. One-Step Pathogen Specific DNA Extraction from Whole Blood on a Centrifugal Microfluidic Device. *Lab. Chip* **2007**, *7*, 565.
- 10. Atencia, J.; Beebe, D.J. Magnetically-Driven Biomimetic Micro Pumping Using Vortices. *Lab. Chip* **2004**, *4*, 598.
- 11. Maruo, S.; Inoue, H. Optically Driven Viscous Micropump Using a Rotating Microdisk. *Appl. Phys. Lett.* **2007**, *91*, 084101.

- 12. Leach, J.; Mushfique, H.; di Leonardo, R.; Padgett, M.; Cooper, J. An Optically Driven Pump for Microfluidics. *Lab. Chip* **2006**, *6*, 735.
- 13. Manz, A.; Effenhauser, C.S.; Burggraf, N.; Harrison, D.J.; Seiler, K.; Fluri, K. Electroosmotic Pumping and Electrophoretic Separations for Miniaturized Chemical Analysis Systems. *J. Micromechanics Microengineering* **1994**, *4*, 257–265.
- 14. Wang, C.; Wang, L.; Zhu, X.; Wang, Y.; Xue, J. Low-Voltage Electroosmotic Pumps Fabricated from Track-Etched Polymer Membranes. *Lab. Chip* **2012**, *12*, 1710.
- 15. Wang, T.; Ni, Q.; Crane, N.; Guldiken, R. Surface Acoustic Wave Based Pumping in a Microchannel. *Microsyst. Technol.* **2017**, 23, 1335–1342.
- 16. Huang, P.-H.; Nama, N.; Mao, Z.; Li, P.; Rufo, J.; Chen, Y.; Xie, Y.; Wei, C.-H.; Wang, L.; Huang, T.J. A Reliable and Programmable Acoustofluidic Pump Powered by Oscillating Sharp-Edge Structures. *Lab. Chip* **2014**, *14*, 4319–4323.
- 17. Ozcelik, A.; Aslan, Z. A Practical Microfluidic Pump Enabled by Acoustofluidics and 3D Printing. *Microfluid. Nanofluidics* **2021**, *25*, 5.
- 18. Lin, Y.; Gao, Y.; Wu, M.; Zhou, R.; Chung, D.; Caraveo, G.; Xu, J. Acoustofluidic Stick-and-Play Micropump Built on Foil for Single-Cell Trapping. *Lab. Chip* **2019**, *19*, 3045–3053.
- 19. Chen, X.; Zhang, C.; Liu, B.; Chang, Y.; Pang, W.; Duan, X. A Self-Contained Acoustofluidic Platform for Biomarker Detection. *Lab. Chip* **2022**, *22*, 3817–3826.
- 20. Kiebert, F.; Wege, S.; Massing, J.; König, J.; Cierpka, C.; Weser, R.; Schmidt, H. 3D Measurement and Simulation of Surface Acoustic Wave Driven Fluid Motion: A Comparison. *Lab. Chip* **2017**, *17*, 2104–2114.
- 21. Bachman, H.; Huang, P.-H.; Zhao, S.; Yang, S.; Zhang, P.; Fu, H.; Huang, T.J. Acoustofluidic Devices Controlled by Cell Phones. *Lab. Chip* **2018**, *18*, 433–441.
- 22. Dentry, M.B.; Friend, J.R.; Yeo, L.Y. Continuous Flow Actuation between External Reservoirs in Small-Scale Devices Driven by Surface Acoustic Waves. *Lab Chip* **2014**, *14*, 750–758.
- 23. Rife, J.C.; Bell, M.I.; Horwitz, J.S.; Kabler, M.N.; Auyeung, R.C.Y.; Kim, W.J. Miniature Valveless Ultrasonic Pumps and Mixers. *Sens. Actuators Phys.* **2000**, *86*, 135–140.
- 24. Tovar, A.R.; Patel, M.V.; Lee, A.P. Lateral Air Cavities for Microfluidic Pumping with the Use of Acoustic Energy. *Microfluid. Nanofluidics* **2011**, *10*, 1269–1278.
- 25. Bachman, H.; Fu, H.; Huang, P.-H.; Tian, Z.; Embry-Seckler, J.; Rufo, J.; Xie, Z.; Hartman, J.H.; Zhao, S.; Yang, S.; et al. Open Source Acoustofluidics. *Lab. Chip* **2019**, *19*, 2404–2414.
- 26. Du, X.Y.; Fu, Y.Q.; Luo, J.K.; Flewitt, A.J.; Milne, W.I. Microfluidic Pumps Employing Surface Acoustic Waves Generated in ZnO Thin Films. *J. Appl. Phys.* **2009**, *105*, 024508.
- 27. Destgeer, G.; Sung, H.J. Recent Advances in Microfluidic Actuation and Micro-Object Manipulation via Surface Acoustic Waves. *Lab. Chip* **2015**, *15*, 2722–2738.
- 28. Huang, A.; Connacher, W.; Stambaugh, M.; Zhang, N.; Zhang, S.; Mei, J.; Jain, A.; Alluri, S.; Leung, V.; Rajapaksa, A.E.; et al. Practical Microcircuits for Handheld Acoustofluidics. *Lab. Chip* **2021**, *21*, 1352–1363.
- 29. Novelli, F.; Hoberg, C.; Adams, E.M.; Klopf, J.M.; Havenith, M. Terahertz Pump–Probe of Liquid Water at 12.3 THz. *Phys. Chem. Chem. Phys.* **2022**, *24*, 653–665.
- 30. Ding, X.; Li, P.; Lin, S.-C.S.; Stratton, Z.S.; Nama, N.; Guo, F.; Slotcavage, D.; Mao, X.; Shi, J.; Costanzo, F.; et al. Surface Acoustic Wave Microfluidics. *Lab. Chip* **2013**, *13*, 3626.
- 31. Hintermüller, M.A.; Jakoby, B.; Reichel, E.K. Acoustic Streaming via a Flexible PCB for Micropumping Applications. *Procedia Eng.* **2016**, *168*, 856–859.
- 32. Connacher, W.; Zhang, N.; Huang, A.; Mei, J.; Zhang, S.; Gopesh, T.; Friend, J. Micro/Nano Acoustofluidics: Materials, Phenomena, Design, Devices, and Applications. *Lab. Chip* **2018**, *18*, 1952–1996, doi:10.1039/C8LC00112J.

- 33. Mohanty, S.; Siciliani de Cumis, U.; Solsona, M.; Misra, S. Bi-Directional Transportation of Micro-Agents Induced by Symmetry-Broken Acoustic Streaming. *AIP Adv.* **2019**, *9*, 035352.
- 34. Nama, N.; Huang, P.-H.; Huang, T.J.; Costanzo, F. Investigation of Acoustic Streaming Patterns around Oscillating Sharp Edges 2014.
- 35. Zhang, C.; Guo, X.; Brunet, P.; Costalonga, M.; Royon, L. Acoustic Streaming near a Sharp Structure and Its Mixing Performance Characterization. *Microfluid. Nanofluidics* **2019**, 23, 104.
- 36. Zhang, C.; Guo, X.; Royon, L.; Brunet, P. Unveiling of the Mechanisms of Acoustic Streaming Induced by Sharp Edges. *Phys. Rev. E* **2020**, *102*, 043110.
- 37. Ovchinnikov, M.; Zhou, J.; Yalamanchili, S. Acoustic Streaming of a Sharp Edge. *J. Acoust. Soc. Am.* **2014**, *136*, 22–29.
- 38. Pavlic, A.; Harshbarger, C.L.; Rosenthaler, L.; Snedeker, J.G.; Dual, J. Sharp-Edge-Based Acoustofluidic Chip Capable of Programmable Pumping, Mixing, Cell Focusing, and Trapping. *Phys. Fluids* **2023**, *35*, 022006, doi:10.1063/5.013992.
- 39. Wu, Z.; Cai, H.; Ao, Z.; Nunez, A.; Liu, H.; Bondesson, M.; Guo, S.; Guo, F. A Digital Acoustofluidic Pump Powered by Localized Fluid-Substrate Interactions. *Anal. Chem.* **2019**, *91*, 7097–7103.
- 40. Collins, D.J.; Manor, O.; Winkler, A.; Schmidt, H.; Friend, J.R.; Yeo, L.Y. Atomization off thin water films generated by high-frequency substrate wave vibrations. *Phys. Rev. E* **2012**. *86*. 056312.
- 41. Kurosawa, M.; Watanabe, T.; Futami, A.; Higuchi T. Surface acoustic wave atomizer. *Sensors and Actuators A: Physical* **1995**, *50*, 69–74.
- 42. Winkler, A.; Harazim, S.; Collins, D.J.; Brünig, R.; Schmidt H.; Menzel S.B. Compact SAW aerosol generator. *Biomedical Microdevices* **2017**, *19*, 9.
- 43. Ranganathan, N.; Li, C.; Suder, T.; Karanji, A.K.; Li, X.; He, Z.; Valentine, S.J.; Li, P. Capillary Vibrating Sharp-Edge Spray Ionization (CVSSI) for Voltage-Free Liquid Chromatography-Mass Spectrometry. *J. Am. Soc. Mass Spectrom.* **2019**, *30*, 824–831.
- 44. Wang, J.; Li, C.; Li, P. A Small Footprint and Robust Interface for Solid Phase Microextraction and Mass Spectrometry Based on Vibrating Sharp-Edge Spray Ionization. *J. Am. Soc. Mass Spectrom.* **2022**, *33*, 304–314.
- 45. Pursell, M.E.; Sharif, D.; DeBastiani, A.; Li, C.; Majuta, S.; Li, P.; Valentine, S.J. Development of CVSSI-APCI for the Improvement of Ion Suppression and Matrix Effects in Complex Mixtures. *Anal. Chem.* **2022**, *94*, 9226–9233.
- 46. Li, C.; Attanayake, K.; Valentine, S.J.; Li, P. Facile Improvement of Negative Ion Mode Electrospray Ionization Using Capillary Vibrating Sharp-Edge Spray Ionization. *Anal. Chem.* **2020**, 92, 2492–2502.
- 47. Li, X.; Attanayake, K.; Valentine, S.J.; Li, P. Vibrating Sharp-edge Spray Ionization (VSSI) for Voltage-free Direct Analysis of Samples Using Mass Spectrometry. *Rapid Commun. Mass Spectrom.* **2021**, *35*.